Proceedings of the 4th International Congress APMAS2014, April 24-27, 2014, Fethiye, Turkey

Cr and V Substitution in the $LiMn_2O_4$Spinel Positive Electrode Li-Ion Batteries

A. Akbulut[b], T. Cetinkaya[a], M.O. Guler[a], M. Uysal[a], H. Akbulut[a,*]

[a]Sakarya University, Metallurgy and Materials Engineering, Esentepe Campus, 54187 Sakarya, Turkey

[b]Sakarya University, Dept. of Environmental Engineering, Esentepe Campus, 54187 Sakarya, Turkey

In this study, $LiCr_{0.2}V_{0.4}Mn_{1.4}O_4$ cathode active electrode materials were produced via a facile sol-gel method at 800°C. The surfaces of the $LiCr_{0.2}V_{0.4}Mn_{1.4}O_4$ cathode active electrode materials were then coated with Cu in order to increase the conductivity and suppress the manganese ion dissolution into the electrolyte. The structure and electrochemical properties of the obtained Cr and V substituted $LiMn_2O_4$ powders were investigated by X-ray diffraction (XRD), scanning electron microscopy (SEM), galvanostatic charge- discharge test and electrochemical impedance spectroscopy (EIS). The improvement in the cycling performances attributed to stabilization of spinel structure by bication ion substation and Cu coating on the spinel particles. EIS analysis confirmed that bication doping and conductive Cu coating contributed stability of the spinel electrodes and provided stable electrolyte/electrode interface due to the suppression of electrolyte decomposition

DOI: 10.12693/APhysPolA.127.1019

PACS: 82.47.Aa, 81.20.Fw, 81.15.–z

1. Introduction

It is well known that, when spinel $LiMn_2O_4$ cathode electrode for Li-ion batteries over discharged at the 3 V level, a structural transformation from cubic spinel phase to tetragonal rock-salt phase will happen, i.e., the so called Jahn-Teller distortion, and results in a fast fading of capacity [1, 2]. The capacity fading of pristine $LiMn_2O_4$ is strongly influenced from Jahn–Teller distortion occurring on the surface of the particles and manganese dissolution into the electrolyte, especially at elevated temperatures. To overcome these drawbacks, two strategies were mainly pursued: elements substitution or oxygen excess to increase the oxidation state of Mn for suppressing the Jahn-Teller effect and surface modification or coating for suppressing the dissolution of Mn into the electrolyte [3]. The first strategy of doping is known to be an effective route. It is reported that substitution of Mn ions with other metals such as Mg, Al, Cr, Co, Ni, Zn, Mg, Ga slows dissolution of Mn into the electrolyte [4]. Partial replacing Mn, could increase the average valence of Mn in $LiMn_2O_4$ (decreasing the Mn^{3+} in $LiMn_2O_4$), and could supress the Jahn-Teller effect [5]. The present work is focused on the understanding of bication effect of (Cr^{3+} and V^{5+}) substituted on $LiMn_2O_4$ cathode in addressing the hampering issues that are concerned with the unacceptable capacity fade and the poor cycle life behavior of spinel cathode. Particularly, after the work of Jayaprakash *et al.* [6], this is the second ever attempt made to explore the electrochemical characteristics of V^{5+} dopant in association with the Cr^{3+} dopant in $LiMn_2O_4$ spinel cathode. To the best of our knowledge, the effect of conductive Cu metal coating on the $LiMn_2O_4$ has not been studied yet.

2. Experiment details

$LiMn_2O_4$ and its substituted spinel $LiCr_{0.2}V_{0.4}Mn_{1.4}O_4$ were prepared by a solution based gel method from a stoichiometric mixture of lithium acetate ($Li(CH_3COO)\cdot 4H_2O$), manganese acetate ($Mn(CH_3\text{-}COO)_2 \cdot 4H_2O$) and metal ion sources such as vanadium pentadionate ($C_{15}H_{21}O_6V$) and chromium nitrate ($Cr(H_2O)_6)(NO_3)_3 \cdot 3H_2O$). The mixture was dissolved in distilled water into which the solution of acetate and ethanol was added drop wise under continuous stirring. pH controlled at ~ 8 with ammonium hydroxide ($NH_3\cdot HO$) addition. The prepared solution was heated at 80°C to evaporate the water until a transparent gel was obtained. The resulting gel was decomposed at 400°C for 5 h in air to remove the organic contents. The heat treated precursor was ground to a fine powder and calcined at 800°C in air for 10 h to obtain the final spinel product. Cu plating on the spinel powders was carried out at 30°C in a container with ultrasonic bath by using a copper sulphate solution of 28 g/L $CuSO_4{:}5H_2O$. Powder X-ray diffraction (XRD) using D/Max-2200 Rigaku (Japan) with CuK_α (λ =1.54178Å) monochromated radiation was performed to identify the crystalline phase of the samples. XRD data were collected in the 2θ ranges from 10° to 80°. The particle size and morphology were investigated by scanning electron microscopy (Jeol 6060 LV). The mixture was composed of 70 wt.% active material, 20 wt.% acetylene black and 10 wt.% polyvinylidene fluoride in a N-methylpyrrolidinone solvent. Coin-type (CR2016) test cells were assembled in an argon-filled glove box, directly using the $LiCr_{0.2}V_{0.4}Mn_{1.4}O_4$ as the working electrode, a lithium metal foil as the counter electrode, a micro porous polypropylene (PP) membrane

*corresponding author; e-mail: akbulut@sakarya.edu.tr

as the separator, and 1M solution of $LiPF_6$ in ethylene carbonate (EC) and dimethyl carbonate (DMC) (1:1 by weight) as the electrolyte. The cells were aged for 12 h before measurements. The cells were cyclically tested on a MTI Model BST8-MA electrochemical analyzer using different current densities over a voltage range of 3–4.3 V. EIS measurements were performed on an electrochemical workstation (Gamry Instrument Reference 300). Impedance spectra of the pristine, doped and copper-coated samples were tested at the open circuit potential. The amplitude of the AC signal was 5 mV over a frequency range from 100 kHz to 10 mHz.

3. Results and discussions

The typical XRD patterns of pristine $LiMn_2O_4$ doped spinel $LiCr_{0.2}V_{0.4}Mn_{1.4}O_4$ are shown in Fig. 1. The XRD patterns of the pristine and doped $LiMn_2O_4$ particles present eight characteristic peaks (Fig. 1a and 1b). Only spinel phase is observed, and it is indicated that the modification does not change the spinel structure of $LiMn_2O_4$. But due to atom size effect it can slightly change the lattice parameters [4]. The lattice parameters were calculated by the least-squares method using 10 diffraction lines. The lattice parameters for the pristine and Cr-V substituted spinels were calculated as 8.247 Å, 8.096 Å, respectively. In order to determine the effects of Cu coating, the XRD were carried out for uncoated and coated spinel materials and presented in Fig. 1c and Fig. 1d according to the JCPDS 04-0836 and JCPDS 98-0094, respectively. As the surfaces of the pristine and $LiCr_{0.2}V_{0.4}Mn_{1.4}O_4$ cathode electrode materials are coated with copper (111) and (221) planes were disappeared. However, no significant change is observed for the (551), (441) and (531) planes after coating with copper when compared with the uncoated pristine $LiCr_{0.2}V_{0.4}Mn_{1.4}O_4$ spinels. However the intensities of the peaks were reduced after coating the surfaces of the based spinels uniformly with copper which is an expected result.

The particle morphologies of the pure $LiMn_2O_4$ and $LiV_{1.4}Cr_{0.2}Mn_{0.4}O_4$ cathode electrode materials powder are shown in Fig. 2a and 2b. As shown in Fig. 2a, the pristine $LiMn_2O_4$ powders annealed at 800°C has a uniform crystalline shape and the average size of particles is 200–300 nm with homogeneous distribution. Additionally, the particles exhibit distinctive visible interference fringes, which indicate good crystallinity. All of the as-prepared cubic spinel powders have nearly polyhedron structure morphology with approximately narrow size distribution. The polyhedron particle sizes for the un-doped spinel are between 0.8 and 1.4 μm with a few smaller particles [7]. From the Fig. 2b, it can be concluded that the substituted samples show a slightly smaller particle size and a more regular morphology than the pristine $LiMn_2O_4$. In addition, the particles of $LiCr_{0.2}V_{0.4}Mn_{1.4}O_4$ samples are distributed more uniformly than those of $LiMn_2O_4$. Fig. 2c and 2d

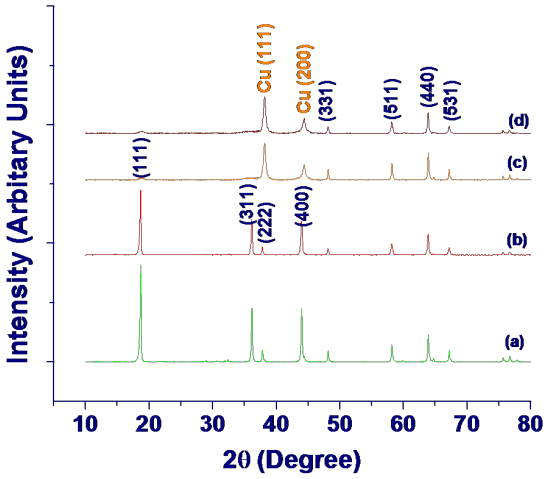

Fig. 1. XRD spectra of the (a) pristine $LiMn_2O_4$ (b) substituted spinel $LiCr_{0.2}V_{0.4}Mn_{1.4}O_4$, (c) $Cu/LiMn_2O_4$ and (d) $Cu/LiCr_{0.2}V_{0.4}Mn_{1.4}O_4$ cathode active electrodes.

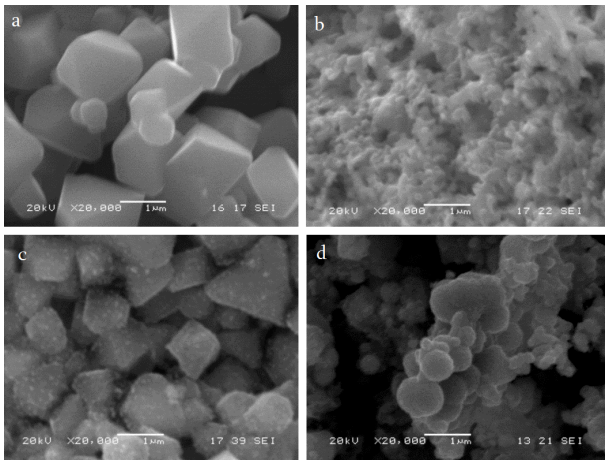

Fig. 2. SEM images of the (a) pristine $LiMn_2O_4$ (b) substituted spinel $LiCr_{0.2}V_{0.4}Mn_{1.4}O_4$, (c) $Cu/LiMn_2O_4$ and $Cu/LiCr_{0.2}V_{0.4}Mn_{1.4}O_4$ cathode active electrodes.

show the SEM images of Cu-coated as-synthesized pristine $LiMn_2O_4$ and substituted $LiMn_2O_4$ powders. No free copper particles and uncoated surface of pristine $LiMn_2O_4$ and substituted $LiMn_2O_4$ particles are found on powders.

The galvanostatic charge and discharge test results are shown in shown in Fig. 3a, 3b, 3c and 3d for pristine, Cr and V doped spinel, Cu coated pristine and Cu coated Cr and V doped spinels, respectively. The cycling tests were performed between 3–4.3 V because of the electrolyte decomposition above 4.3 V. The capacities obtained correspond to the oxidation of Mn^{3+} to Mn^{4+} and M^{3+}/M^{4+} (where M is Cr and V). As can be concluded from the Fig. 3a, pristine spinel exhibited a specific capacity of 109 mA h g^{-1}. However, by introducing Cr and V ions

as a replacement for Mn^{3+} ions give a remarkably higher capacity (136 mA h g^{-1}) as shown in Fig. 3b. Introducing Cr and V into spinel structure, the oxidation of a similar amount of Mn^{3+} to the Mn^{4+} state lead to an increase in the average oxidation state of manganese. The diminished Mn^{3+} ion concentration causes a reduction in the unit-cell volume of the spinel, which results in increased structural stability. The capacities obtained correspond to oxidation of Mn^{3+} to Mn^{4+} [8]. The cyclic performances of Cu coated spinels for the first, second and fiftieth cycles were also shown in Fig. 3c and 3d. The initial charge curves of Cu coated samples show a shorter plateau compared to pristine sample, leading to lower initial charge capacity. This can be attributed to the strong mechanical bonding with the Cu with pristine samples, which suppress the oxygen vacancies migration and reduce the activity of the evolved oxygen species, leading to less oxygen removal and less electrolyte oxidation during the initial charge process [9]. Table I summarizes the

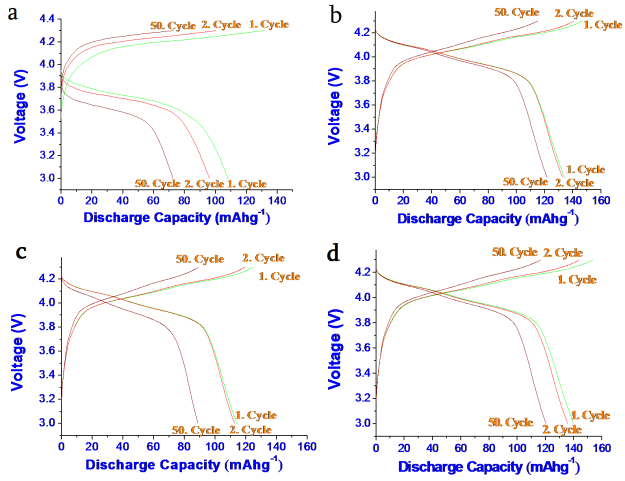

Fig. 3. Galvanostatic charge and discharge tests of the (a) pristine $LiMn_2O_4$ (b) substituted spinel $LiCr_{0.2}V_{0.4}Mn_{1.4}O_4$, (c) $Cu/LiMn_2O_4$ and (d) $Cu/LiCr_{0.2}V_{0.4}Mn_{1.4}O_4$ cathode active electrodes.

cyclic performance of the four cathode electrodes at a constant rate of 1C and shows the cycling performance of the Cr and V substituted spinel was significantly improved. The content of Mn^{3+} within the spinel structure is decreased and as a result Jahn-Teller distortion, which damages the structural integrity of the electrode during charge/discharge cycling and results in rapid capacity fading is suppressed [10].

The electrochemical impedance spectroscopies are performed to investigate the variation of electrode resistance of $LiMn_2O_4$ samples. The Nyquist plots of the $LiMn_2O_4$ samples after the first charge–discharge cycle are shown in Fig. 4b. The charge transfer resistance values obtained from the equivalent circuit for pristine $LiMn_2O_4$, $LiCr_{0.2}V_{0.4}Mn_{1.4}O_4$, $Cu/LiMn_2O_4$ and $Cu/LiCr_{0.2}V_{0.4}Mn_{1.4}O_4$ were 564 Ω, 455 Ω, 266 Ω and 250 Ω, respectively.

Summary of electrochemical performance of pristine $LiMn_2O_4$, $LiV_{1.4}Cr_{0.2}Mn_{0.4}O_4$, Cu coated $LiMn_2O_4$, and Cu coated $LiV_{1.4}Cr_{0.2}Mn_{0.4}O_4$ spinel cathode active electrodes TABLE I

Samples	Discharge capacity (mA h g^{-1})			Capacity fading (%)
	1^{st} Cycle	2^{nd} Cycle	50^{th} Cycle	
$LiMn_2O_4$	109	97	72	34
$LiCr_{0.2}V_{0.4}Mn_{1.4}O_4$	136	133	118	13
Cu coated $LiMn_2O_4$	117	115	88	31
Cu coated $LiCr_{0.2}V_{0.4}Mn_{1.4}O_4$	141	137	119	16

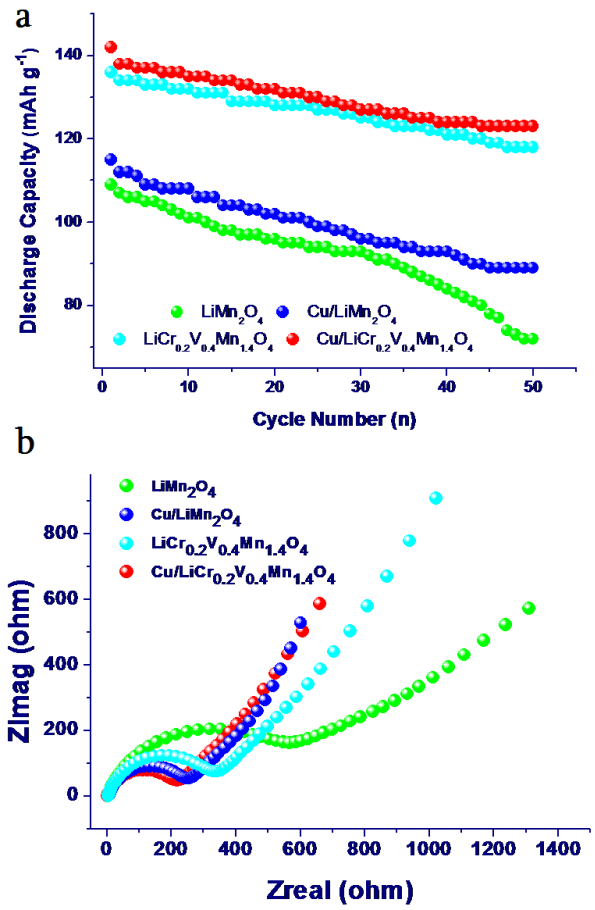

Fig. 4. (a) Galvanostatic discharge vs cycling number curves and (b) EIS spectra of spinel cathode active electrodes.

4. Conclusions

Spinel based pristine $LiMn_2O_4$, and $LiCr_{0.2}V_{0.4}Mn_{1.4}O_4$ powders have been synthesized via facile sol-gel method, and the spinel powders were successfully coated with metallic Cu via electroless deposition techniques. The XRD results all

synthesized cathode active electrodes are identified as a single phase of cubic spinel structure. The Cu coated $LiCr_{0.2}V_{0.4}Mn_{1.4}O_4$ powders exhibited low charge transfer resistance (R_{ct}), accompanying the best electrochemical activity and highest discharge capacity. Substituting Mn with Cr and V provided remarkably high discharge capacities. The initial discharge capacity of Cu coated $LiCr_{0.2}V_{0.4}Mn_{1.4}O_4$ was 141 $mA\,h\,g^{-1}$ and the capacity fade was only 16% after 50 cycles. The considerably large capacity may originate from preventing to Jahn–Teller distortion and Mn dissolution during electrochemical reactions. This work opens up a facile and effective route for the synthesis of double doping $LiMn_2O_4$ with the excellent electrochemical performance.

Acknowledgments

This work is supported by the Scientific and Technological Research Council of Turkey (TUBITAK) under the contract number 111M021. The authors thank the TUBITAK MAG workers for their financial support.

References

[1] M. Aklalouch, J.M. Amarilla, R.M. Rojas, I. Saadoune, J.M. Rojo, *J. Power Sources* **185**, 501 (2008).

[2] W. Xu, A. Yuan, L. Tian, Y. Wang, *J. Appl. Electrochem.* **41**, 453 (2011).

[3] H.B. Sun, Y.G. Chen, C.H. Xu, D. Zhu, L.H. Huang, *J. Solid State Electrochem.* **16**, 1247 (2012).

[4] C. Wang, S. Lu, S. Kan, J. Pang, W. Jin, X. Zhang, *J. Power Sources* **189**, 607 (2009).

[5] Y. Kim, J. Lim, S. Kang, *Inter. J. Quantum Chemistry* **113**, 148 (2013).

[6] N. Jayaprakash, N. Kalaiselvi, G. Babu, D. Bhuvaneswari, *J. Solid State Electrochem.* **15**, 1243 (2011).

[7] M.O. Guler, A. Akbulut, T. Cetinkaya, M. Uysal, H. Akbulut, *Int. J. Hydrogen Energy* **39**, 21447 (2014).

[8] D. Ke, Y. Fei, H. Guorong, D.P. Zhong, C. Yanbing, S.R. Kwang, *J. Power Sources* **244**, 29 (2013).

[9] A. Mohamed, M.A. Jose, S. Ismael, M.R. Jose, *J. Power Sources* **196**, 10222 (2011).

[10] M.T. Rajive, K.K.M. Anil, P.B. Anand, S. Jayalekshmi, *J. Physics and Chemistry of Solids* **72**, 1251 (2011).